

# Fabrication, structure and properties of quasi-carbon fibres

LIREN ZHAO, BOR Z. JANG\*

Center for Materials Research and Education, 204 Wilmore Laboratory, Auburn University, AL 36849, USA

Partially carbonized fibres, termed quasi-carbon fibres (QCF), with good thermal stability and acceptable mechanical properties were developed from a polyacrylonitrile-based precursor. Heat treatment temperature (HTT), in the 400–950 °C range, played a major role in determining the thermal, mechanical and electrical properties of the QCF. The thermal stability of the QCF was increased by increasing the HTT. An appreciable amount of the graphite-like structure in QCF began to develop at ca. 650 °C. The Young modulus magnitudes of QCF scaled almost linearly with the pyrolysis temperature. In contrast, the QCF exhibited a decreasing trend in both tensile strength and failure strain up to a HTT of 650 °C, above which both the tensile strength and failure strain of the QCF increased with the HTT. Electrical resistivity values of the QCF covered a very wide range from  $10^7$  to  $10^{-2}$  Ω cm. QCF showed semiconducting behaviours with activation energies falling between 0.690 and 0.0052 eV when the pyrolysis temperature was in the 400–850 °C range.

## 1. Introduction

Carbon fibres have been extensively used as reinforcement materials to provide high strength and stiffness in advanced composites [1–4]. The preparation of carbon fibres normally involves a high heat treatment temperature (HTT),  $> 1000$  °C, which provides carbon fibres with good mechanical and electrical conducting properties. Relatively fewer research efforts have been concentrated on treating fibres at temperatures  $< 1000$  °C to produce partially carbonized fibres. Recently, interests in these partially carbonized fibres have been increasing [5–7] because they exhibit unique physical and chemical properties. Goldberg *et al.* [8] have reported that partially pyrolysed fibres show an interesting electrical switching behaviour. Pitch-based and rayon-based partially carbonized fibres were regarded as promising materials for use in thermal-type infrared detectors [9]. Polyacrylonitrile (PAN)-based partially carbonized fibres have been developed in our laboratory and used in the fabrication of high-performance composites. These materials cover a wide spectrum of thermal, electrical and mechanical properties. A complete characterization of these PAN-based fibres is essential to understanding the relationships between the structure and properties of these fibres and their resulting composites.

The fabrication of carbon fibres from a PAN precursor usually involved two steps [1, 2]. The pre-oxidation or stabilization of PAN fibre precursors is generally regarded as a crucial first step to assure good

quality carbon fibres. The low temperature treatment (200–300 °C) converted PAN to an infusible ladder structure [10, 11]. After stabilization, the oxidized PAN fibre (OXPAN) can be further treated at a higher temperature. Instead of obtaining conventional carbon fibres at a temperature  $> 1000$  °C, partially carbonized products can be prepared in the 400–950 °C range in an inert atmosphere. The structure of the fibre would experience a dramatic change with gradual loss of non-carbon elements and condensation of benzene rings during partial carbonization. Thus, the properties of these pyrolysed intermediate fibres [or quasi-carbon fibres (QCF)] can be tailored by simply varying the heat treatment parameters (temperature, time and heating rate). Therefore, the aims of the present work were to study the effect of the pyrolysis temperature and time on the properties of QCF and to provide a better understanding of how structure variations are related to thermal, electrical and mechanical behaviours of QCF.

## 2. Experimental procedure

PAN-based copolymer fibres used for the preparation of QCF were received in the form of a tow containing 6 K filaments of 1.1 denier and 11.5 μm average diameter. The precursor was stabilized in air in the 210–230 °C range for 2.5 h while under tension to avoid shrinkage. Differential scanning calorimetry (DSC) was employed to characterize the degree of stabilization and to determine optimal conditions for

\* To whom all correspondence should be directed.

the oxidation treatment. Various QCF samples were fabricated by pyrolysis of the OXPAN fibre in an argon atmosphere between 400 and 950 °C for three different durations of time (1, 3 and 6 h). The heating rate used to raise a sample to the desired treatment temperature was 3 °C min<sup>-1</sup>. For comparison, carbon fibre was also prepared from the OXPAN fibre at a HTT of 1200 °C.

The density of the QCF was measured by the density gradient column method. A density gradient of 0.867–1.989 g cm<sup>-3</sup> was obtained in a 1.5 m long glass tube by using a mixture of toluene and 1,3-dibromopropane. Since some QCF filaments were not uniform in the cross-section area, the diameter (*D*) of filaments was determined from density (Equation 1) rather than from microscopic measurements:

$$D = \{4w/\pi d\}^{1/2} \quad (1)$$

where *w* is the weight per unit length of a single QCF filament and *d* is the fibre density.

The microstructure of the OXPAN fibre and QCF were determined by a Rigaku wide-angle X-ray diffractometer with a CuK<sub>α</sub> radiation source. The “Aromatization index” [12] was used to define the degree of stabilization of the OXPAN fibre:

$$AI = I_a/(I_a + I_p) \quad (2)$$

where *I<sub>a</sub>* and *I<sub>p</sub>* are the diffraction intensity values of the ladder structure at  $\theta = 25$  and  $17^\circ$ , respectively. The stacking size (*L<sub>c</sub>*) of the QCF was calculated from the half-width (*B*) of the (002) reflection, using the Scherrer formula:

$$L_c = k\lambda/B\cos\theta \quad (3)$$

where  $\lambda = 0.154$  nm,  $\theta$  is the Bragg angle and *k* is a constant (ca. 1.0). The crystallinity of QCF was also characterized by the relative intensity of the peak at  $\theta = 25^\circ$ . The pyrolysis-induced structural changes of QCF were studied with a Mattson Polaris FTIR spectrometer, using the powered fibre samples pressed with anhydrous KBr to form transparent films.

A Perkin-Elmer TGA-7 thermal analyser was employed to study the dynamic thermal stability of QCF, using a heating rate of 20 °C min<sup>-1</sup> from 30 to 850 °C and an air flow rate of 80 cm<sup>3</sup> min<sup>-1</sup>. The weight of each sample for TGA measurement was ca. 3 mg.

Tensile tests with a gauge length of 5 cm and a crosshead speed of 0.5 mm min<sup>-1</sup> were used to characterize the mechanical behaviour of QCF. Fibres measured were in bundle form and were slightly impregnated with the epoxy resin. At least 10 samples of each QCF were used to obtain the average values of tensile strength and modulus. The texture and cross-section of QCF after the tensile test were examined with a scanning electron microscope (SEM).

The electrical resistance of QCF was measured by the four-probe method. The pyro-resistance effect was used to evaluate the semiconducting characteristic and the activation energy (*E<sub>a</sub>*) for the conduction mechanism of QCF:

$$\ln \rho = \rho_0 + E_a/kT \quad (4)$$

where  $\rho$  is the electrical resistivity at the absolute temperature *T* (K), *k* is the Boltzmann constant and  $\rho_0$  is a material constant.

### 3. Results and discussion

#### 3.1. Basic parameters

Fig. 1 shows the density variation of QCF with the HTT. The density of the PAN fibre was 1.18 g cm<sup>-3</sup> while that of OXPAN fibre was 1.37 g cm<sup>-3</sup>, the latter being higher due to the oxygen atoms absorbed by the fibre during the stabilization stage to form a cyclic ladder structure. The density of QCF increased very rapidly with increasing HTT (when HTT < 650 °C), but gradually levelled off when reaching 650 °C. The result was similar to that reported by Ko *et al.* [13]. At the early stage of carbonization, the ladder structure in the OXPAN fibre underwent cross-linking condensation by dehydrogenation to form the embryonic carbon basal planes that have a more compact structure than the precursor. When the pyrolysis temperature reached ca. 650 °C, denitrogenation became dominant in broadening and lengthening these small basal planes to form a graphite-like structure. During carbonization, fibres tended to shrink in both longitudinal and transverse directions, releasing non-carbon elements as volatile gases. Therefore, both diameter and length of QCF decreased with the increasing HTT, as seen in Figs 2 and 3, respectively. It can also be concluded from Figs 1 and 2 that the pyrolysis time was less crucial than the pyrolysis temperature (HTT) in dictating the structure and properties of QCF.

#### 3.2. Microstructure

##### 3.2.1. X-ray diffraction (XRD) studies

The XRD patterns of QCF heat treated from 400 to 1200 °C for 1 h are shown in Fig. 4. The characteristic diffraction peak of the PAN fibre precursor appeared at  $2\theta = 17^\circ$ . After stabilization, a new peak developed at  $2\theta = 25^\circ$ , which was related to the ladder structure of the OXPAN fibre forming an essentially amorphous structure. According to Equation 2, the *AI* value of the OXPAN fibre was calculated to be 87.1%.

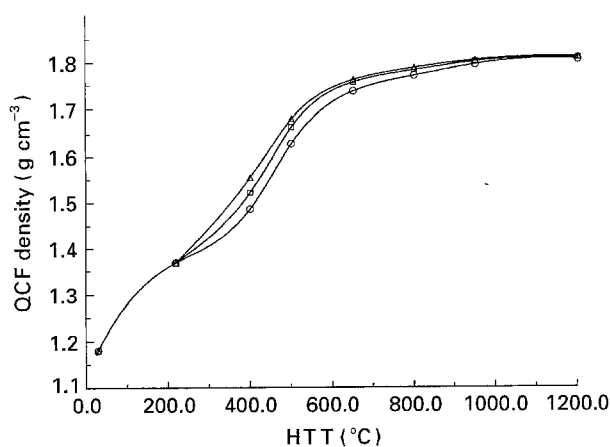


Figure 1 The variation of QCF density versus HTT. ○, 1 h; □, 3 h; △, 6 h.

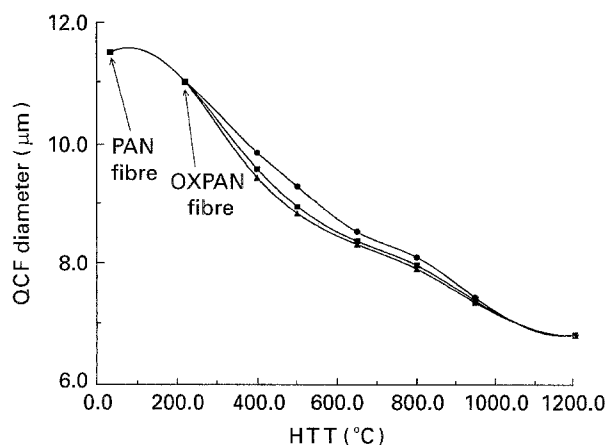


Figure 2 The variation of QCF filament diameter with HTT. ●, 1 h; ■, 3 h; ▲, 6 h.

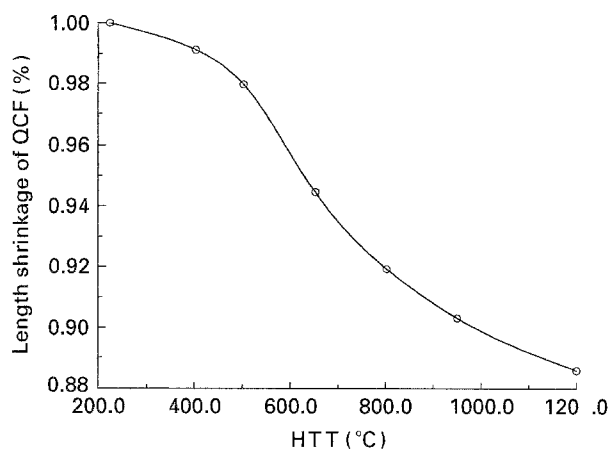


Figure 3 The length shrinkage of QCF heat treated for 1 h as a function of HTT.

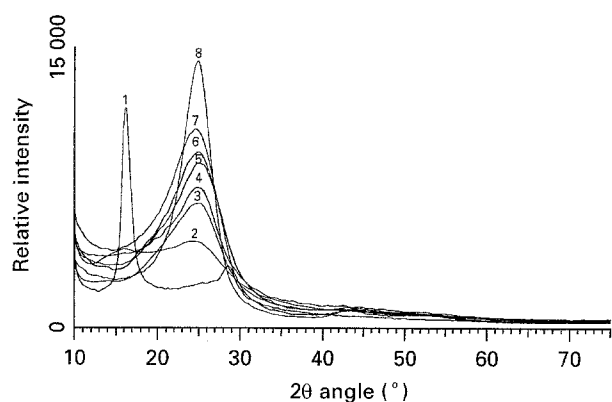


Figure 4 XRD patterns of QCF heat treated at various temperatures for 1 h. 1, PAN fibre; 2, OXPAN fibre; 3, QCF-400; 4, QCF-500; 5, QCF-650; 6, QCF-800; 7, QCF-950; 8, carbon fibre.

When the HTT was raised, the Bragg angle remained almost unchanged, but the peak of QCF, corresponding to (002) diffraction in the graphite-like structure, became more intense and the old peak at  $2\theta = 17^\circ$  gradually disappeared. Meanwhile, the half-width of the peak ( $B$ ) at  $2\theta = 25^\circ$  was reduced with a higher HTT. These observations imply that the stacking size ( $L_c$ ) as well as the crystallinity of QCF increased during carbonization (Table I).

TABLE I XRD results of the QCF heat treated at various temperatures for 1 h.

HTT (°C)	400	500	650	800	950	1200
$2\theta$ (degree)	25.2	25.0	25.0	25.1	25.1	25.3
Half-width ( $B$ , °)	7.8	7.6	7.3	7.1	6.8	4.2
Stacking size ( $L_c$ , nm)	1.16	1.19	1.24	1.27	1.38	2.15
Relative intensity	7230	7627	9242	9428	10770	14370

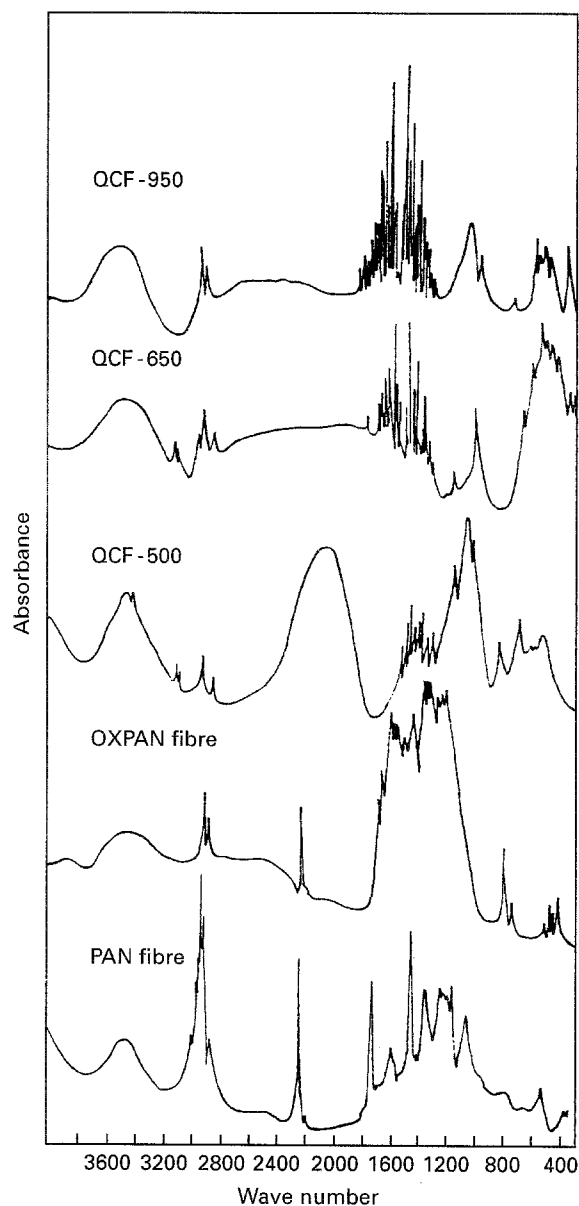


Figure 5 I.r. Spectra of fibres.

### 3.2.2. FTIR studies

FTIR spectra of fibres pyrolysed at different temperatures for 1 h are presented in Fig. 5. The cyano ( $-\text{CN}$ ) groups in the PAN fibre appeared at  $2245\text{ cm}^{-1}$ . Upon stabilization,  $-\text{CN}$  groups at  $2241\text{ cm}^{-1}$  became weaker and  $-\text{C}=\text{N}-$  groups appeared at  $1571\text{ cm}^{-1}$  in the OXPAN fibre, reflecting the formation of a cyclic polypyrrole-like structure. Further rising of the pyrolysis temperature led to the

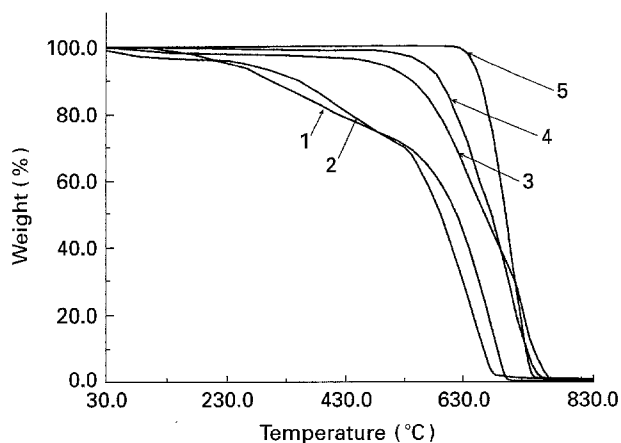


Figure 6 TGA curves of fibres. 1, PAN fibre; 2, PANOX fibre; 3, QCF-400; 4, QCF-500; 5, QCF-950.

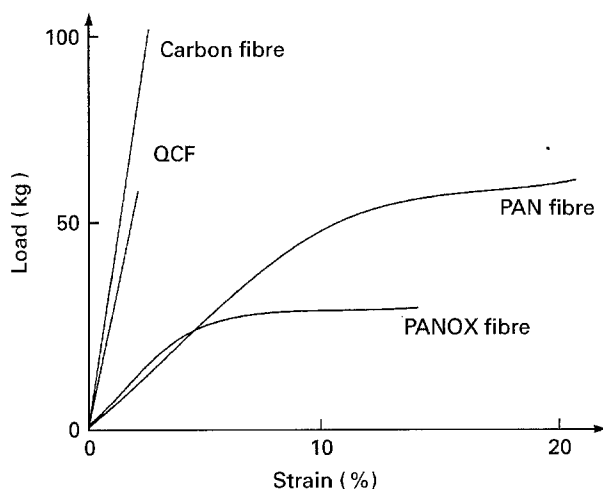


Figure 7 Comparison of schematic load-displacement curves among fibres.

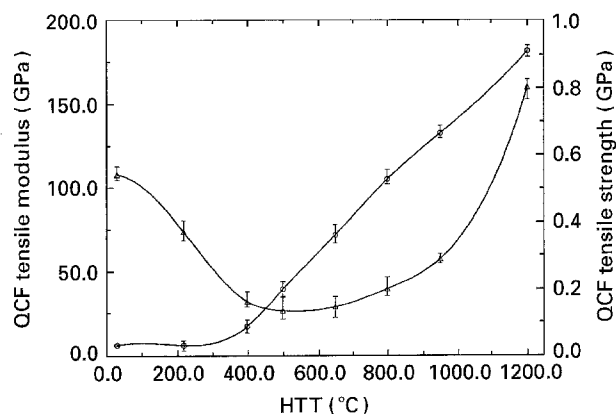


Figure 8 The variation of modulus and strength of QCF with HTT.  $\Delta$ , Strength;  $\circ$ , modulus.

disappearance of the  $-\text{CN}$  peak and the gradual appearance of a new peak ca.  $2219\text{ cm}^{-1}$ , which was believed to reflect a complex structure in QCF-400 and QCF-500 (OXPAN fibre pyrolysed at 400 and 500  $^{\circ}\text{C}$ , respectively). At ca. 650  $^{\circ}\text{C}$ , the fibre began to form a more complete aromatic, graphite-like molecular structure. The i.r. spectra of QCF with a HTT  $> 650\text{ }^{\circ}\text{C}$  were virtually unchanged from those of

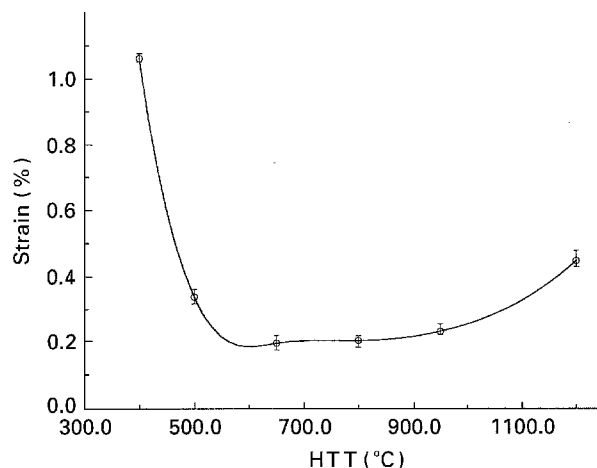


Figure 9 The variation of strain to failure of QCF with HTT. Break strain of: PAN fibre, 21.49%; OXPAN, 10.82%.

carbon fibres. Thus, the graphite-like structure in QCF is believed to begin to develop at a HTT of ca. 650  $^{\circ}\text{C}$ .

### 3.3. Thermal stability

Fig. 6 illustrates the results of thermogravimetric analysis (TGA) by using the dynamic thermal scan mode on the PAN, OXPAN and QCF pyrolysed at different temperatures for 1 h. Mass loss of the PAN fibre appeared at 260  $^{\circ}\text{C}$  due to cyclization of the original PAN structure. The mass loss onset temperature of the OXPAN fibre was at 330  $^{\circ}\text{C}$ , which was considered to be associated with oxidation degradation. The mass loss of QCF began at a higher temperature ( $> 450\text{ }^{\circ}\text{C}$ ) and increased with the increasing pyrolysis temperature due to the formation of a more ordered structure. Thus, QCF exhibited good thermal stability even though they were heat treated at relatively low carbonization temperatures.

### 3.4. Mechanical properties

Fig. 7 schematically illustrates the tensile load-displacement curves of the fibres studied. Both PAN and OXPAN fibres exhibited relatively low Young moduli and ductile behaviours, while QCF showed relative high Young moduli and brittle characteristics. The variation in tensile strength and modulus of QCF with HTT are summarized in Fig. 8. The modulus of QCF increased with increasing HTT and a nearly linear relationship between the modulus and the temperature was observed after 400  $^{\circ}\text{C}$ . This trend may be attributed to an increase in the crystalline stacking size and the orientation of the fused aromatic structure along the fibre axis. Thus, the average modulus value of pyrolysed fibres changed from 16.5 GPa for QCF-400 to 133.4 GPa for QCF-950. In contrast, a parabola-like curve was observed in the tensile strength diagram, which was quite similar to the result obtained in polymeric carbon materials after partial carbonization [14]. At the early stage of carbonization, QCF showed a decreasing trend in strength, being quite weak up to ca. 500–650  $^{\circ}\text{C}$ . Above 650  $^{\circ}\text{C}$ ,

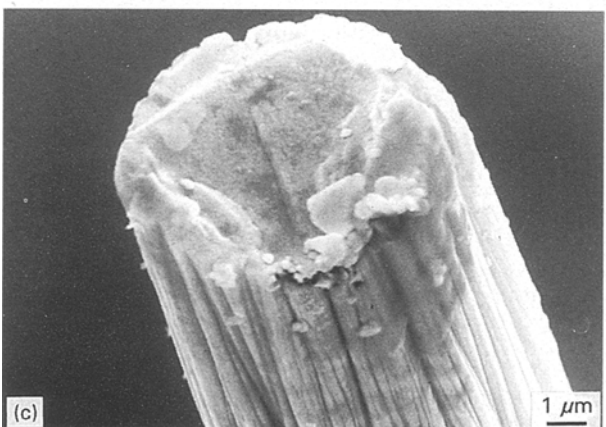
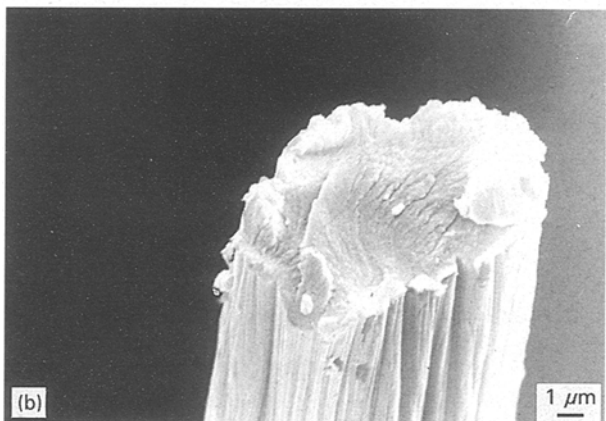
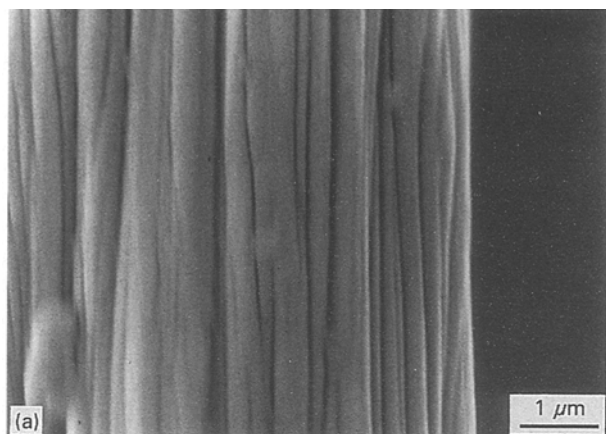


Figure 10 SEM micrographs of: (a) texture of QCF; (b) QCF-400 after tensile test; (c) QCF-650 after tensile test.

the tensile strength of QCF increased rapidly with increasing pyrolysis temperature. Cracks are often considered to be the main factor that affects the strength of materials. When the OXPAN fibre was pyrolysed, the ladder structure was gradually condensed to leave flaws among the embryonic basal planes, thereby decreasing the strength. When the HTT reached 650 °C, a graphite-like structure began to form that was characterized by extended carbon basal planes. More covalent bonds were also formed to bridge aromatic layers in the direction perpendicular to the carbon basal planes, leading to the subsequent increase in strength. Therefore, QCF that are pyrolysed ca. 500–650 °C showed the minimum strength.

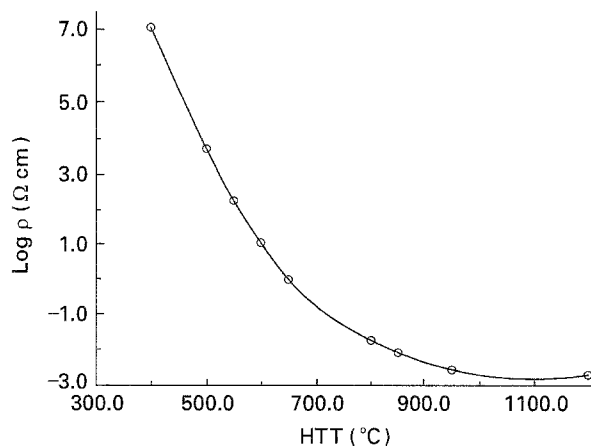


Figure 11 Electrical resistivity of QCF as a function of HTT.

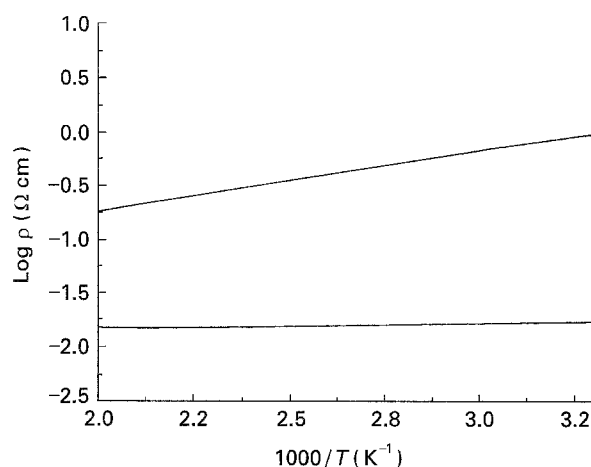


Figure 12 Temperature dependence of electrical resistivity of QCF-650 (top line) and QCF-800 (bottom line).

A similar curve was observed in the diagram of tensile failure strain of QCF versus HTT, as indicated in Fig. 9. A low failure strain value also existed at a temperature of ca. 650 °C. OXPAN fibres still retained a relatively ductile behaviour with a failure strain of 10.82%, but the brittleness of QCF increased drastically during the initial partial carbonization up to a HTT of 650 °C. A decrease in brittleness may be related to the increased strength, since both brittleness and strength are dictated by the internal defects which are HTT dependent. Thus, less brittle characteristics of QCF could be observed at pyrolysis temperatures > 650 °C.

Fig. 10 illustrates SEM observations of the surface texture and the cross-section area of QCF. The striations along the fibre axis on the fibre surface can be clearly seen (Fig. 10a). After tensile testing, the QCF with a lower HTT (e.g. QCF-400) showed a rougher or more ductile cross-section (Fig. 10b), while the QCF heat treated at a higher temperature (e.g. QCF-650) exhibited a smoother cross-section area reflecting the brittle behaviour (Fig. 10c). Flaws can also be seen in the micrographs. These results are consistent with the tensile property data.

### 3.5. Electrical properties

Fig. 11 shows the variation in electrical resistivity of QCF as a function of the HTT. The conductivity of

TABLE II Temperature dependence in the activation energy ( $E_a$ ) of various QCF heat treated for 1 h

HTT (°C)	400	500	600	650	800	850	950
$E_a$ (eV)	0.690	0.348	0.185	0.116	0.0155	0.0052	-0.0312

the OXPAN fibres was still in the insulator range. A typically semiconducting behaviour ( $\rho$  value  $10^7$ – $10^{-2}$   $\Omega$  cm) was observed for QCF prepared with a HTT in the 400–800 °C range. When the HTT exceeded ca. 800 °C, changes in electrical resistivity of these pyrolysed fibres became less dramatic. This behaviour is consistent with the observed structural changes as stated earlier, i.e., large aromatic, sheet-like basal planes were developed at high temperatures leading to the extended mean free paths of electrons in a graphite-like structure. The temperature dependence of electrical resistance of QCF (e.g., QCF-650 and QCF-800) was almost linear in the measured temperature range, as seen in Fig. 12. The pyro-resistance effect in these QCF was remarkable; a negative temperature coefficient was observed with the fibres treated at 400–850 °C. Calculations according to Equation 4 showed that the activation energy ( $E_a$ ) for the conduction mechanism in QCF was approximately in the range of 0.690–0.005 eV when the HTT was in the 400–850 °C range. This notion further confirmed that these QCF exhibited semi-conducting behaviours. When the HTT was  $> 950$  °C, QCF exhibited the metal-like characteristics with a negative  $E_a$  value. The activation energy data of various QCF are summarized in Table II.

#### 4. Conclusions

1. Quasi-carbon fibres with semiconducting characteristics, good thermal stability and acceptable mechanical properties have been fabricated from a PAN-based precursor in the 400–950 °C range. The property changes were mainly dictated by the heat treatment temperature.
2. The formation of the graphite-like structure in QCF began at ca. 650 °C according to FTIR studies. Experimental data also confirmed that the HTT ca. 650 °C served as a turning point at which the properties of QCF changed dramatically.
3. XRD patterns of QCF indicated that the stacking size ( $L_c$ ), as well as the crystallinity, of QCF increased with the HTT during the partial carbonization. Changes were more pronounced when the HTT was  $> 650$  °C.
4. The modulus magnitudes of QCF scaled almost linearly with the pyrolysis temperature, but the

QCF exhibited a decreasing trend in tensile strength and failure strain up to a HTT of 650 °C. After 650 °C, the tensile strength and failure strain of the QCF began to rise with the increasing HTT.

5. Electrical resistivity values of these QCF covered a very wide spectrum, ranging from  $10^7$  to  $10^{-2}$   $\Omega$  cm. A semiconducting behaviour with the activation energy lying in the 0.690–0.005 eV range was obtained when the pyrolysis temperature was 400–850 °C.

#### Acknowledgements

Financial supports provided by the NSF Materials Engineering and Tribology Program and the NSF/AL-EPSCOR program are gratefully acknowledged.

#### References

1. A. K. GUPTA, D. K. PALIWAL and P. BAJAJ, *J. Mater. Sci. – Rev. Macromol. Chem. Phys.* **C31** (1991) 1.
2. S. DAMODARAN, P. DESAI and A. S. ABHIRAMAN, *J. Text. Inst.* **81** (1990) 384.
3. G. HENRICI-OLIVÈ and S. OLIVÈ, *Adv. Polymer Sci.* **51** (1983) 1.
4. P. RAJALINGAM and G. RADHAKRISHNAN, *J. Mater. Sci. Rev. Macromol. Chem. Phys.* **C31** (1991) 301.
5. J. G. VENNEN and Y. S. KO, US Patent 4 938 941 (1990).
6. G. PAN, N. MUTO, M. MIYAYAMA and H. YANAGIDA, *J. Mater. Sci.* **27** (1992) 3497.
7. *Idem.*, *J. Mater. Sci. Lett.* **12** (1993) 666.
8. H. A. GOLDBERG, I. L. KALNIN, C. C. WILLIAMS and I. L. SPAIN, US Patent 4 642 664 (1987).
9. N. MUTO, M. MIYAYAMA, H. YANAGIDA, N. MORI, T. KAJIWARA, Y. IMAI, A. URANO and H. ICHIKAWA, *Sensors and Mater.* **2** (1991) 313.
10. P. J. GOODHEW, A. J. CLARKE and J. E. BAILEY, *Mater. Sci. Engng.* **17** (1975) 3.
11. M. K. JAIN, M. BALASUBRAMANIAN, P. DESAI and A. S. ABHIRAMAN, *J. Mater. Sci.* **22** (1987) 301.
12. T. UCHIDA, I. SHINOYAMA, Y. ITO and K. NAKUDA in Proceedings of the 10th Biennial Conference on Carbon (Bethlehem, PA, 1977) p. 31.
13. T. H. KO, T. C. DAY and J. A. PERNG, *Carbon* **31** (1993) 765.
14. T. H. KO and K. W. HONE, *Sampe J.* **28** (1992) 17.

Received 8 September 1994  
and accepted 23 February 1995